

A review of the theory of incompressible MHD turbulence

Benjamin D. G. Chandran (benjamin-chandran@uiowa.edu) *

Department of Physics & Astronomy, University of Iowa

Abstract. This brief review provides an introduction to key ideas in the theory of incompressible magnetohydrodynamic (MHD) turbulence.

1. Introduction

Magnetohydrodynamic (MHD) turbulence has been studied in a number of different parameter regimes, with important contributions from many authors, including [1–41]. This review focuses on incompressible turbulence in which the fluctuating velocities are comparable to or less than the Alfvén speed [defined in equation (7)]. It is assumed that there is a mean magnetic field \mathbf{B}_0 that is at least as strong as the turbulent magnetic-field fluctuations. Sections 2 and 3 review the MHD equations and MHD waves, and section 4 describes wave-wave interactions. Section 5 reviews results on weak MHD turbulence, and section 6 treats strong MHD turbulence. Section 7 describes the role of dynamic alignment in the decay of MHD turbulence.

2. Equations of incompressible MHD

The governing equations of incompressible MHD are

$$\rho \left(\frac{\partial \mathbf{v}}{\partial t} + \mathbf{v} \cdot \nabla \mathbf{v} \right) = -\nabla \left(p + \frac{B^2}{8\pi} \right) + \frac{1}{4\pi} \mathbf{B} \cdot \nabla \mathbf{B} + \rho \nu \nabla^2 \mathbf{v}, \quad (1)$$

$$\frac{\partial \mathbf{B}}{\partial t} = \nabla \times (\mathbf{v} \times \mathbf{B}) + \eta \nabla^2 \mathbf{B}, \quad (2)$$

$$\nabla \cdot \mathbf{B} = 0, \quad (3)$$

$$\nabla \cdot \mathbf{v} = 0, \quad (4)$$

and

$$\rho = \text{constant}, \quad (5)$$

where \mathbf{B} is the magnetic field, \mathbf{v} is the velocity, p is the thermal pressure, ρ is the density, and ν is the viscosity. In the limit $\eta \rightarrow 0$, equation (2)

* The author acknowledges the support of NSF grant AST-0098086 and DOE grants DE-FG02-01ER54658 and DE-FC02-01ER54651 at the University of Iowa.



implies that field lines are like threads that are frozen to the plasma and advected at the plasma velocity \mathbf{v} .

Upon defining

$$\mathbf{B} = B_0 \hat{\mathbf{z}} + \delta \mathbf{B}, \quad (6)$$

where $B_0 \hat{\mathbf{z}}$ is the uniform mean field,

$$\mathbf{b} = \frac{\mathbf{B}}{\sqrt{4\pi\rho}} = v_A \hat{\mathbf{z}} + \delta \mathbf{b}, \quad (7)$$

where $v_A = B_0/\sqrt{4\pi\rho}$ is the Alfvén speed, the Elsasser variables

$$\mathbf{a}^\pm = \mathbf{v} \pm \delta \mathbf{b}, \quad (8)$$

and the total pressure

$$\Pi = \frac{p}{\rho} + \frac{b^2}{2}, \quad (9)$$

and upon neglecting the dissipation terms ($\nu = \eta = 0$), equations (1) and (2) can be rewritten as

$$\frac{\partial \mathbf{a}^+}{\partial t} - v_A \frac{\partial \mathbf{a}^+}{\partial z} = -\nabla \Pi - \mathbf{a}^- \cdot \nabla \mathbf{a}^+, \quad (10)$$

and

$$\frac{\partial \mathbf{a}^-}{\partial t} + v_A \frac{\partial \mathbf{a}^-}{\partial z} = -\nabla \Pi - \mathbf{a}^+ \cdot \nabla \mathbf{a}^-. \quad (11)$$

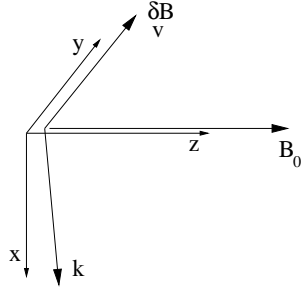
In the absence of dissipation, equations (1) through (5) possess three quadratic invariants: the energy $(1/2) \int (v^2 + b^2) d^3x$, the cross helicity $(1/2) \int \mathbf{v} \cdot \delta \mathbf{b} d^3x = (1/8) \int (\mathbf{a}^+ \cdot \mathbf{a}^+ - \mathbf{a}^- \cdot \mathbf{a}^-) d^3x$, and the magnetic helicity $\int \mathbf{A} \cdot \mathbf{B} d^3x$, where \mathbf{A} is the magnetic vector potential. The magnetic helicity measures linkages of magnetic field lines and is associated with an inverse cascade [3]. The cross helicity describes the excess of one fluctuation type (\mathbf{a}^+ or \mathbf{a}^-) over the other, and is associated with the phenomenon of dynamic alignment (section 7).

3. Waves and wave packets in incompressible MHD

If $\mathbf{v} = \delta \mathbf{b}$ (i.e., $\mathbf{a}^- = 0$), the solution to equation (10) for $\nabla \times \mathbf{a}^+$ is a wave that travels at speed v_A in the $-z$ direction. Similarly, if $\mathbf{v} = -\delta \mathbf{b}$ (i.e., $\mathbf{a}^+ = 0$), the solution to equation (11) for $\nabla \times \mathbf{a}^-$ is a wave that travels at speed v_A in the $+z$ direction. These wave solutions are valid for arbitrarily large wave amplitude (when either $\mathbf{a}^+ = 0$ or $\mathbf{a}^- = 0$).

There are two types of waves in incompressible MHD, the Alfvén wave and the slow wave, with polarizations illustrated in figure 1. Both

ALFVEN-WAVE POLARIZATION



SLOW-WAVE POLARIZATION

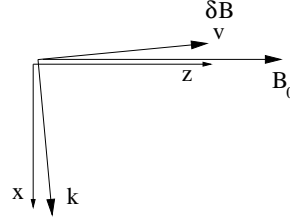


Figure 1. For an Alfvén wave, $\delta\mathbf{v}$ and $\delta\mathbf{B}$ are \perp to both \mathbf{B}_0 and the wave vector \mathbf{k} . For a slow wave, $\delta\mathbf{v}$ and $\delta\mathbf{B}$ are \perp to \mathbf{k} , but in the plane of \mathbf{k} and \mathbf{B}_0 . If \mathbf{k} is nearly \perp to \mathbf{B}_0 , then $\delta\mathbf{v}$ and $\delta\mathbf{b}$ are nearly along \mathbf{B}_0 for a slow wave.

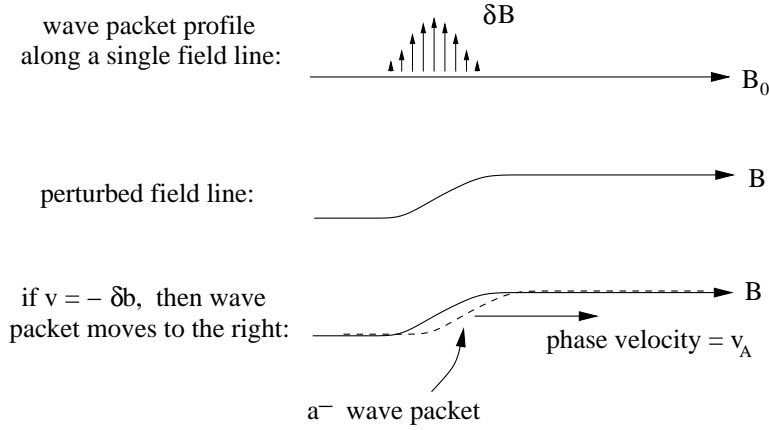


Figure 2. The profile of a 1D Alfvén wave packet.

waves propagate along (or anti-parallel to) \mathbf{B}_0 at speed v_A . A 1D \mathbf{a}^- -Alfvén-wave-packet (with $\mathbf{v} = -\delta\mathbf{b}$) is illustrated in figure 2. A cubical portion of a 3D wave packet is illustrated in figure 3.

In general, a wave packet is associated with a displacement $\Delta\mathbf{r}$ of a field line, as in figures 2 and 3. For a small-amplitude wave packet that perturbs the field lines only slightly,

$$\Delta\mathbf{r} = \frac{1}{B_0} \int_{-\infty}^{\infty} \mathbf{B}_{\perp}(z) dz = \frac{\tilde{\mathbf{B}}_{\perp}(k_z = 0)}{B_0}, \quad (12)$$

where \mathbf{B}_{\perp} is the component of $\delta\mathbf{B}$ in the xy -plane, and $\tilde{\mathbf{B}}_{\perp}$ is the Fourier transform of \mathbf{B}_{\perp} in z . Thus, the field-line displacement is given

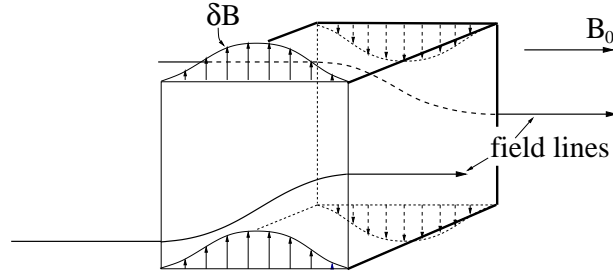


Figure 3. An example of a cubical portion of a 3D wave packet.

by the $k_z = 0$ component of a wave packet. [16] If an Alfvén wave packet’s length along the field is λ_{\parallel} , its width across the field is λ_{\perp} , and its amplitude is $B_{\lambda_{\perp}}$, then equation (12) implies that

$$\Delta r \sim \frac{\lambda_{\parallel} B_{\lambda_{\perp}}}{B_0} \sim \frac{\lambda_{\parallel} a_{\lambda_{\perp}}}{v_A}, \quad (13)$$

where $a_{\lambda_{\perp}}$ is the wave-packet amplitude in Elsasser variables.

4. Wave-wave interactions in incompressible MHD

For the nonlinear $\mathbf{a}^{\pm} \cdot \nabla \mathbf{a}^{\mp}$ terms in equations (10) and (11) to be nonzero, both \mathbf{a}^+ and \mathbf{a}^- fluctuations must be present at the same point in space. Wave-wave interactions can thus be thought of as collisions between oppositely directed wave packets [2]. When \mathbf{a}^+ and \mathbf{a}^- wave packets collide, to lowest order in wave amplitude each wave packet follows the field lines associated with the other wave packet [11, 29]. For example, before a collision the value of \mathbf{a}^- remains constant at a point that moves along \mathbf{B}_0 at speed v_A . During the collision, the value of \mathbf{a}^- remains approximately constant at a point that moves at speed $\sim v_A$ along the field lines formed from the sum of \mathbf{B}_0 and the field fluctuations of the \mathbf{a}^+ wave packet, with a pressure-induced correction to ensure $\nabla \cdot \mathbf{a}^- = 0$ [29]. This is illustrated in figure 4 for cubical portions of two colliding wave packets. In both cubes, $\delta \mathbf{B}$ is upwards in the near-face of the cube, and downward in the rear-face of the cube, as in figure 3.

The different displacements of different parts of a wave packet during a collision shear the wave packet in the plane perpendicular to \mathbf{B}_0 . For colliding wave packets of length λ_{\parallel} along \mathbf{B}_0 and width λ_{\perp} across \mathbf{B}_0 ,

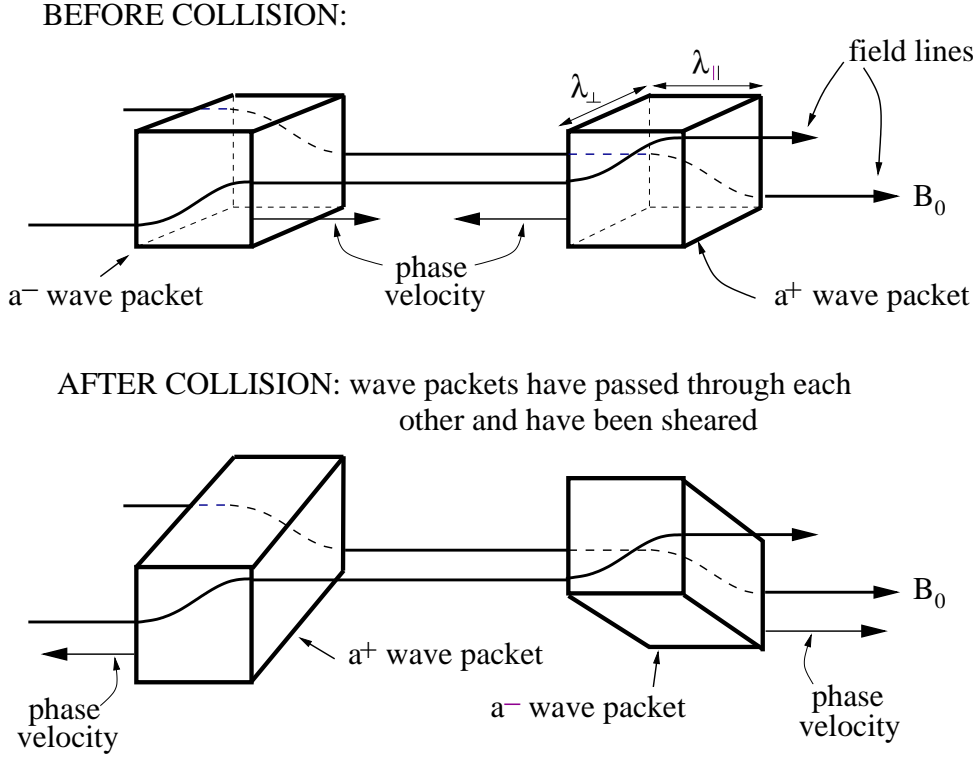


Figure 4. During a wave-packet collision, the \mathbf{a}^- (\mathbf{a}^+) packet follows the field lines of the \mathbf{a}^+ (\mathbf{a}^-) packet.

the change in the value of \mathbf{a}^\pm induced by the collision is roughly the duration of a collision, λ_{\parallel}/v_A , times the magnitude of the nonlinear $\mathbf{a}^\mp \cdot \nabla \mathbf{a}^\pm$ term. If $|\mathbf{a}^+| \sim |\mathbf{a}^-| \sim a_{\lambda_{\perp}}$, and if $\lambda_{\perp} \lesssim \lambda_{\parallel}$, then the fractional change χ in \mathbf{a}^\pm induced by the collision is given by [13]

$$\chi \sim \frac{a_{\lambda_{\perp}} \lambda_{\parallel}}{v_A \lambda_{\perp}}, \quad (14)$$

or, from equation (13),

$$\chi \sim \frac{\Delta r}{\lambda_{\perp}}. \quad (15)$$

When $\chi \ll 1$, the right-hand side of, for example, the \mathbf{a}^- wave packet in figure 4 is displaced in almost the same way as the left-hand side, since both sides encounter essentially the same \mathbf{a}^+ wave packet, since the \mathbf{a}^+ packet is only slightly altered during the collision. Changes to the profile of a wave packet along the magnetic field are thus weaker than changes in the profile of a wave packet in the plane

\perp to \mathbf{B}_0 [8, 17, 18]. As a result, the cascade of energy to small λ_{\parallel} is much less efficient than the cascade of energy to small λ_{\perp} in weak incompressible MHD turbulence, as discussed in the following section.

5. Weak incompressible MHD turbulence

In weak incompressible MHD turbulence, $\chi \ll 1$ and nonlinear wave-wave interactions are a small perturbation to a wave's linear oscillatory behavior. In this limit, the wave kinetic equation for the power spectra can be derived using weak turbulence theory [25]. When only Alfvén waves are excited, the wave kinetic equation is of the form [25]

$$\begin{aligned} \frac{\partial E^{\pm}(\mathbf{k})}{\partial t} = & \int d^3k_1 d^3k_2 [N_{\mathbf{k},\mathbf{k}_1,\mathbf{k}_2} E^{\pm}(\mathbf{k}) - P_{\mathbf{k},\mathbf{k}_1,\mathbf{k}_2} E^{\pm}(\mathbf{k}_1)] E^{\mp}(\mathbf{k}_2) \\ & \times \delta(\omega_{\mathbf{k}}^{\pm} - \omega_{\mathbf{k}_1}^{\pm} - \omega_{\mathbf{k}_2}^{\mp}) \delta(\mathbf{k} - \mathbf{k}_1 - \mathbf{k}_2), \end{aligned} \quad (16)$$

where \mathbf{k} is the Fourier-space wave number,

$$E^{\pm}(\mathbf{k}) \delta(\mathbf{k} + \mathbf{k}_1) = \langle \tilde{\mathbf{a}}^{\pm}(\mathbf{k}) \cdot \tilde{\mathbf{a}}^{\pm}(\mathbf{k}_1) \rangle, \quad (17)$$

$\tilde{\mathbf{a}}^{\pm}$ is the Fourier transform of \mathbf{a}^{\pm} , $\langle \dots \rangle$ indicates an ensemble average, the kernels $N_{\mathbf{k},\mathbf{k}_1,\mathbf{k}_2}$ and $P_{\mathbf{k},\mathbf{k}_1,\mathbf{k}_2}$ are independent of E^{\pm} and given by [25], and

$$\omega_{\mathbf{k}}^{\pm} = \mp k_z v_A \quad (18)$$

is the frequency of small-amplitude \mathbf{a}^{\pm} -waves, from equations (10) and (11). Equation (16) contains only the leading-order terms in the weak-turbulence expansion, called the three-wave-interaction terms. The delta functions in the integrand give the three-wave resonance conditions,

$$\mathbf{k} = \mathbf{k}_1 + \mathbf{k}_2, \quad (19)$$

and

$$\omega_{\mathbf{k}}^{\pm} = \omega_{\mathbf{k}_1}^{\pm} + \omega_{\mathbf{k}_2}^{\mp}. \quad (20)$$

The integrand in equation (16) contains the product $E^{\pm} E^{\mp}$ and no terms of the form $E^{\pm} E^{\pm}$, consistent with the fact that only oppositely directed wave packets interact. Upon dividing equation (20) by v_A , one finds that

$$-k_z = -k_{1z} + k_{2z} \quad (21)$$

Combining equation (21) with the z -component of equation (19) yields

$$k_{2z} = 0, \quad \text{and} \quad k_z = k_{1z}. \quad (22)$$

If turbulence is not excited initially at some value of k_z , three-wave interactions will not excite turbulence at that value of k_z . Indeed, three-wave interactions do not transfer energy to larger values of k_z , only to larger values of $k_\perp = \sqrt{k_x^2 + k_y^2}$ [8, 25]. Also, the rate of energy transfer for E^\pm is in essence proportional to the $k_z = 0$ part of E^\mp . These conclusions remain valid when slow waves are also excited. [25]

What physical meaning can be attributed to the $k_z = 0$ part of the power spectrum? It is simpler to answer this question by working with a 1D spectrum (M , defined below) obtained by integrating E^+ over k_x and k_y . Assuming homogeneous turbulence, let

$$\langle \mathbf{B}^+(x, y, 0) \cdot \mathbf{B}^+(x, y, z) \rangle = g(z), \quad (23)$$

where \mathbf{B}^+ is the fluctuating magnetic field associated with all \mathbf{a}^+ wave packets ($\mathbf{B}^+ = \mathbf{a}^+ \sqrt{\pi\rho}$), and let

$$M(k_z) = \int_{-\infty}^{\infty} e^{-ik_z z} g(z) dz. \quad (24)$$

Equations (17) and (24) imply that $M(k_z) = [\rho/32\pi^4] \int dk_x dk_y E^+(\mathbf{k})$. Assuming that all wave packets have coherence length λ_\parallel along the magnetic field, coherence length λ_\perp across the field, and rms fluctuating field B_{λ_\perp} , one finds that

$$M(0) = \left\langle \int_{-\infty}^{\infty} \mathbf{B}^+(x, y, 0) \cdot \mathbf{B}^+(x, y, z) dz \right\rangle \sim B_{\lambda_\perp}^2 \lambda_\parallel. \quad (25)$$

If the wave packets have the Alfvén-wave polarization, $\delta\mathbf{B} \perp \mathbf{B}_0$, then from equation (13),

$$M(0) \sim B_{\lambda_\perp} B_0 \Delta r, \quad (26)$$

where $\Delta r \sim B_{\lambda_\perp} \lambda_\parallel / B_0$ is the field-line displacement associated with a single wave packet. Thus, for Alfvén waves, $M(0)$ [and similarly $E^\pm(k_z = 0)$] is a measure of the field-line displacements caused by wave packets. The dependence of the cascade rate on $E^\mp(k_z = 0)$ indicates that energy cascade arises from the turbulent wandering of field lines, as described in section 4. [16–18, 30, 41] As illustrated by equation (26), the $k_z = 0$ part of the spectrum should not be equated with wave packets that have infinite coherence length along the magnetic field [32, 41]; structures with finite λ_\parallel lead to nonzero Δr , $M(0)$, and $E(k_z = 0)$.

The power spectrum of weak incompressible MHD turbulence can be estimated as follows [17, 18, 25, 28]. The fractional change χ in a wave packet of width λ_\perp and length λ_\parallel during one collision is $\ll 1$. Since the changes induced by successive collisions add randomly, χ^{-2} collisions are required for an order-unity fractional change. The time

required for χ^{-2} collisions is $\chi^{-2}\lambda_{\parallel}/v_A$, or $\sim v_A\lambda_{\perp}^2/(a_{\lambda_{\perp}}^2\lambda_{\parallel})$. This is roughly the time τ_{cascade} required for eddies of width λ_{\perp} to pass their energy to eddies of width $\sim \lambda_{\perp}/2$. The cascade power ϵ is roughly the energy per unit mass in wave packets of width λ_{\perp} , i.e. $a_{\lambda_{\perp}}^2/2$, divided by τ_{cascade} :

$$\epsilon \sim \frac{a_{\lambda_{\perp}}^4 \lambda_{\parallel}}{v_A \lambda_{\perp}^2}. \quad (27)$$

Assuming that local interactions in wave-number space dominate the cascade, ϵ is independent of λ_{\perp} when $\lambda_{\perp} \ll l$ and $\lambda_{\perp} \gg d$, where l is the outer scale (stirring scale) and d is the dissipation scale. Since λ_{\parallel} is effectively constant,

$$a_{\lambda_{\perp}} \propto \lambda_{\perp}^{1/2} \quad (28)$$

[17, 18, 25]. If the one-dimensional power spectrum $E_{1D}(k_{\perp})$ is defined so that the energy of modes with k_{\perp} in the interval $(k_1, 2k_1)$, i.e. $a_{k_1}^2$, is given by $\int_{k_1}^{2k_1} E_{1D}(k_{\perp}) dk_{\perp} \sim k_1 E_{1D}(k_1)$, then

$$E_{1D}(k_{\perp}) \propto k_{\perp}^{-2} \quad (29)$$

[17, 18, 25].

Inserting equation (28) into equation (14) yields [18]

$$\chi \propto \lambda_{\perp}^{-1/2}. \quad (30)$$

Thus, if the dissipation scale d is sufficiently small, then at sufficiently small λ_{\perp} the value of χ increases to 1, and the turbulence becomes strong.

6. Strong incompressible MHD turbulence

In strong MHD turbulence, for which $\chi \gtrsim 1$, fluctuations are not waves, since they are significantly distorted by nonlinear interactions during a single wave period. Nor can propagation of fluctuations along the magnetic field be ignored, since, for example, for $\chi \sim 1$ propagation is in some sense equally important as wave-wave interactions. The combination of propagation and nonlinear interaction determines the length of eddies in strong incompressible MHD turbulence as follows. [13, 29, 30]

Consider a volume of width λ_{\perp} across the magnetic field and length λ_{\parallel} along the field, with $\lambda_{\parallel} \gg \lambda_{\perp}$. The \mathbf{a}^- fluctuations within this volume will be loosely described as a “wave packet” with the label W1. It is useful to consider the “large-scale” magnetic field that is obtained by filtering out all magnetic fluctuations on length scales comparable

to or smaller than $W1$. If one assumes that the dominant nonlinear interactions are between structures of similar size (local in k -space), one can neglect the shearing of $W1$ by the large-scale magnetic field. Within a box that is large compared to $W1$ but small compared to the outer scale l , one can thus approximate the large-scale magnetic field as a uniform mean field denoted $\mathbf{B}_{\text{local}}$, as in figure 5. From equation (11), $W1$ propagates along $\mathbf{B}_{\text{local}}$ at speed $B_{\text{local}}/\sqrt{4\pi\rho}$, while at the same time undergoing nonlinear interactions. Let $W2$ be a “wave packet” of \mathbf{a}^+ fluctuations, also of width λ_{\perp} and length λ_{\parallel} , propagating antiparallel to $\mathbf{B}_{\text{local}}$ while undergoing nonlinear interactions. Let $a_{\lambda_{\perp}}$ be the amplitude of \mathbf{a}^- within $W1$ and also of \mathbf{a}^+ within $W2$. Let $\lambda_{\parallel,\text{crit}}$ be the value of λ_{\parallel} such that $\chi = 1$ for $W1$ and $W2$: $\lambda_{\parallel,\text{crit}} = \lambda_{\perp}v_A/a_{\lambda_{\perp}}$.

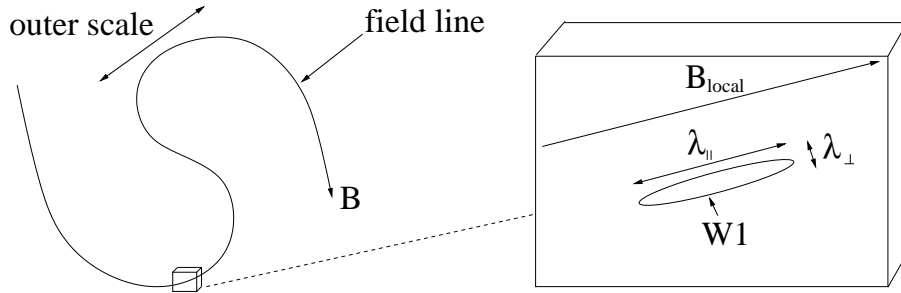


Figure 5. In strong MHD turbulence, eddies are elongated along the local magnetic field.

Let us suppose that $W1$ and $W2$ collide, and that $\lambda_{\parallel} \gg \lambda_{\parallel,\text{crit}}$ (i.e. $\chi \gg 1$), so that initially the \mathbf{a}^- and \mathbf{a}^+ fluctuations are coherent over a distance $\gg \lambda_{\parallel,\text{crit}}$ along $\mathbf{B}_{\text{local}}$. After $W1$ and $W2$ have propagated into each other a distance $\lambda_{\parallel,\text{crit}}$, as depicted in the bottom part of figure 6, the \mathbf{a}^- (\mathbf{a}^+) fluctuations at the leading edge of $W1$ ($W2$) above point Q (P) have been altered by a factor of order unity by nonlinear interactions. As time proceeds, the \mathbf{a}^- fluctuations above points P and Q will evolve in different ways, because they are interacting with significantly different \mathbf{a}^+ fluctuations: the \mathbf{a}^- fluctuations above point Q interact with the pristine, undistorted version of $W2$; the \mathbf{a}^- fluctuations above point P interact with \mathbf{a}^+ fluctuations in $W2$ that have already been changed by the collision. As a result, the collision introduces structure with parallel coherence length $\lambda_{\parallel,\text{crit}}$ into the two wave packets.

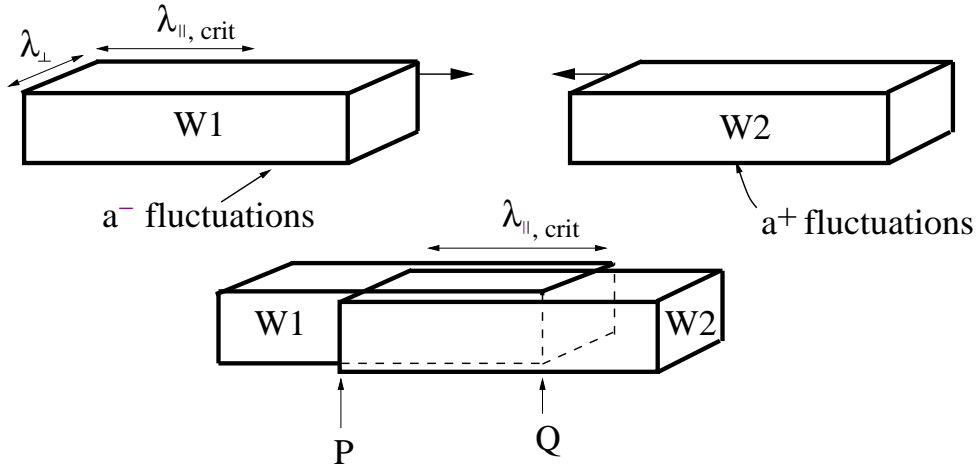


Figure 6.

According to these heuristic arguments, if χ is initially $\gg 1$ (but finite), the combination of nonlinear interaction and propagation along field lines reduces χ until $\chi \sim 1$. On the other hand, weak turbulence theory shows that if χ is initially $\ll 1$, nonlinear interactions act to increase χ until $\chi \sim 1$, as discussed in section 5. Thus, 1 is in some sense the “stable equilibrium value” of χ in incompressible MHD turbulence. [13]

When $\chi \sim 1$, the turbulence is strong. A theory for the spectrum and anisotropy of strong incompressible MHD turbulence was developed by [13]. The time τ_{cascade} for eddies of width λ_{\perp} and length λ_{\parallel} to pass their energy to smaller eddies is $\sim \lambda_{\parallel}/v_A \sim \lambda_{\perp}/a_{\lambda_{\perp}}$. Assuming local interactions in k -space, the cascade power ϵ is given by $a_{\lambda_{\perp}}^2/\tau_{\text{cascade}} \sim a_{\lambda_{\perp}}^3/\lambda_{\perp}$. Assuming that ϵ is independent of λ_{\perp} ,

$$a_{\lambda_{\perp}} \propto \lambda_{\perp}^{1/3}, \quad (31)$$

which corresponds to

$$E_{1D}(k_{\perp}) \propto k_{\perp}^{-5/3}. \quad (32)$$

The condition $\chi \sim 1$ combined with equation (31) yields [13]

$$\lambda_{\parallel} \propto \lambda_{\perp}^{2/3}. \quad (33)$$

If the turbulence is stirred at scale l , and if $a_l \simeq v_A$, then [13]

$$\lambda_{\parallel} = l^{1/3} \lambda_{\perp}^{2/3}. \quad (34)$$

Equations (31) through (34) apply to both Alfvén-mode eddies and slow-mode eddies [13]. However, Alfvén-mode fluctuations dominate

the shearing of both Alfvén-mode eddies and slow-mode eddies [13]. The reason is that the nonlinear $\mathbf{a}^\pm \cdot \nabla \mathbf{a}^\mp$ terms are much larger for Alfvén modes than for slow modes, since fluctuations vary most rapidly across the magnetic field, and \mathbf{a}^\pm is perpendicular to the local magnetic field for Alfvén modes, but nearly along the magnetic field for slow modes when $\lambda_\perp \ll \lambda_\parallel$.

Equations (31) through (34) are consistent with the numerical results of [27, 36]. The numerical simulations of [26] agree with equation (32), but do not address local anisotropy. On the other hand, the numerical simulations of [29] are consistent with equation (34), but find $E_{1D}(k_\perp) \propto k_\perp^{-3/2}$. Thus, although equations (31) through (34) are supported by physical arguments and some direct numerical simulations, areas of uncertainty remain.

7. Decay and dynamic alignment

If only one type of fluctuation, either \mathbf{a}^+ or \mathbf{a}^- , is present, nonlinear interactions vanish. Such a state is called “maximally aligned,” since either $\mathbf{v} = \mathbf{b}$ or $\mathbf{v} = -\mathbf{b}$. Decaying “turbulence” that is maximally aligned decays only on a viscous or resistive time scale, and can thus be long-lived.

If decaying turbulence initially contains both \mathbf{a}^+ and \mathbf{a}^- fluctuations, but an excess of one over the other, then it decays to a maximally aligned state, in which only the initially predominating fluctuation type remains. [4, 6, 9, 25, 29, 36, 41] The reason for this is the following. Whether the turbulence is weak or strong, isotropic or anisotropic, the energy-cascade time of \mathbf{a}^\pm fluctuations at a perpendicular scale λ_\perp is proportional to some power of the energy in \mathbf{a}^\mp fluctuations at scale λ_\perp . If turbulence is excited with an excess of \mathbf{a}^+ waves, the decay time for the \mathbf{a}^- waves is short compared to the decay time of the \mathbf{a}^+ waves. The \mathbf{a}^- waves thus decay faster than the \mathbf{a}^+ fluctuations, with a discrepancy in decay rates that increases in time. It has been suggested by [37] that this mechanism also operates in compressible MHD turbulence, in which case it provides a potential mechanism for long-lived turbulence in astrophysical environments.

References

1. Iroshnikov, P. 1963, *Astron. Zh.*, 40, 742
2. Kraichnan, R. H. 1965, *Phys. Fluids*, 8, 1385
3. Pouquet, A., Frisch, U., & Léorat, J. 1976, *J. Fluid Mech.*, 77, 321
4. Dobrowolny, M., Mangeney, A., & Veltri, P. 1980, *Phys. Rev. Letters*, 45, 144

5. Montgomery, D., & Turner, L. 1981, *Phys. Fluids*, 24, 825
6. Grappin, R., Pouquet, A., Léorat, J. 1983, *Astron. Astrophys.*, 126, 51
7. Higdon, J. C. 1984, *ApJ*, 285, 109
8. Shebalin, J. V., Matthaeus, W., & Montgomery, D. 1983, *J. Plasma Phys.*, 29, 525
9. Ting, A., Matthaeus, W., & Montgomery, D. 1986, *Phys. Fluids*, 29, 3261
10. Zank, G. P., & Matthaeus, W. H. 1993, *Phys. Fluids*, A5, 257
11. Sridhar, S., & Goldreich, P. 1994, *ApJ*, 432, 612
12. Oughton, S., Priest, E., & Matthaeus, W. 1994, *J. Fluid Mech.*, 280, 95
13. Goldreich, P., & Sridhar, S. 1995, *ApJ*, 438, 763
14. Politano, H., Pouquet, A., & Sulem, P.-L. 1995, *Phys. Plasmas*, 2, 2931
15. Montgomery, D., & Matthaeus, W. 1995, *ApJ*, 447, 706
16. Ng, C. S., & Bhattacharjee, A. 1996, *ApJ*, 465, 845
17. Ng, C. S., & Bhattacharjee, A. 1997, *Phys. Plasmas*, 4, 605
18. Goldreich, P., & Sridhar, S. 1997, *ApJ*, 485, 680
19. Ghosh, S., & Goldstein, M. 1997, *J. Plasma Phys.*, 57, 129
20. Stone, J., Ostriker, E., & Gammie, C. 1998, *ApJ*, 508, L99
21. Kinney, R. M., & McWilliams, J. C. 1998, *Phys. Rev. E*, 57, 7111
22. Balsara, D., & Pouquet, A. 1999, *Phys. Plasmas*, 6, 89
23. Mac Low, M. M. 1999, *ApJ*, 524, 169
24. Vazquez-Semadeni, E., Ostriker, E., Passot, T., Gammie, C., & Stone, J. 2000, *Protostars and Planets IV*, eds Mannings, V., Boss, A.P., and Russell, S. (Tucson: University of Arizona Press), p. 3
25. Galtier, S., Nazarenko, S. V., Newell, A. C., & Pouquet, A. 2000, *J. Plasma Phys.*, 63, 447
26. Müller, W., & Biskamp, D., 2000, *Phys. Rev. Lett.*, 84, 475
27. Cho, J., & Vishniac, E. 2000, *ApJ*, 539, 273
28. Bhattacharjee, A., & Ng, N. 2001, *ApJ*, 548, 318
29. Maron, J., & Goldreich, P. 2001, *ApJ*, 554, 1175
30. Lithwick, Y., & Goldreich, P. 2001, *ApJ*, 562, 279
31. Milano, L., Matthaeus, W., Dmitruk, P., Montgomery, D. C. 2001, *Phys. Plasmas*, 8, 2673
32. Galtier, S., Nazarenko, S., Newell, A., & Pouquet, A. 2002, *ApJ*, 564, L49
33. Ossenkopf, V., & Mac Low, M. 2002, *A&A*, 390, 3070
34. Schekochihin, A., Maron, J., & Cowley, S. 2002, *ApJ*, 576, 2002
35. Boldyrev, S., Nordlund, A., & Padoan, P. 2002, *ApJ*, 573, 678
36. Cho, J., Lazarian, A., & Vishniac, E. 2002, *ApJ*, 564, 291
37. Cho, J., & Lazarian, A. 2003, *astro-ph/0301062*
38. Winters, W., Balbus, S., Hawley, J. 2003, *MNRAS*, 340, 519
39. Vestuto, J., Ostriker, E., Stone, J. 2003, *ApJ*, 590, 858
40. Passot, T., & Vazquez-Semadeni, E. 2003, *A&A*, 398, 845
41. Lithwick, Y., & Goldreich, P. 2003, *ApJ*, 582, 1220